



Influence of radiative heat transfer and transverse magnetic field on peristaltic flow of a third order fluid in a planar channel

M. Y. Abdollahzadeh Jamalabadi^{1*}, Mohammad Ebrahimi², Gelareh Homayoun³
and Payam Hooshmand⁴

¹Chabahar Maritime University, Chabahar, Iran

²Department of Management, Mahabad Branch, Islamic Azad University, Mahabad, Iran

³Department of Architect Engineering, Mahabad Branch, Islamic Azad University, Mahabad, Iran

⁴Department of Mechanical Engineering, Mahabad Branch, Islamic Azad University, Mahabad, Iran

ABSTRACT

The influence of radiative heat transfer on peristaltic flow of a third order fluid through the between parallel plate with transverse magnetic field has been studied. The governing equations of two dimensional fluids have been simplified under the consideration of long wavelength and low Reynolds number approximation. Exact analytical calculations are carried out for the pressure gradient, velocity, pressure rise, friction force on the heat transfer rate. The effect of the non-dimensional wave amplitude, the variable magnetic field, the ratio of relaxation of retardation time, the radius ratio and the non-dimensional volume flow are analyzed theoretically and computed numerically. Comparison was made with the results obtained in the presence and absence of variable magnetic field and an endoscope. The results indicate that the effect of the non-dimensional wave amplitude, variable magnetic field, ratio of relaxation to retardation time, radius ratio and non-dimensional volume flow on peristaltic flow is very pronounced.

Keywords: Peristaltic flow; Fractional third grade fluid; Magnetic field; Heat transfer; Analytical solutions

INTRODUCTION

A non-Newtonian fluid is a fluid with properties that differ in any way from those of Newtonian fluids. Most commonly, the viscosity (the measure of a fluid's ability to resist gradual deformation by shear or tensile stresses) of non-Newtonian fluids is dependent on shear rate or shear rate history. Some non-Newtonian fluids with shear-independent viscosity, however, still exhibit normal stress-differences or other non-Newtonian behavior. Many salt solutions and molten polymers are non-Newtonian fluids, as are many commonly found substances such as ketchup, custard, toothpaste, starch suspensions, paint, blood, and shampoo [1]. In a Newtonian fluid, the relation between the shear stress and the shear rate is linear, passing through the origin, the constant of proportionality being the coefficient of viscosity. In a non-Newtonian fluid, the relation between the shear stress and the shear rate is different and can even be time-dependent (Time Dependent Viscosity). Therefore, a constant coefficient of viscosity cannot be defined. Although the concept of viscosity is commonly used in fluid mechanics to characterize the shear properties of a fluid, it can be inadequate to describe non-Newtonian fluids. They are best studied through several other rheological properties that relate stress and strain rate tensors under many different flow conditions—such as oscillatory shear or extensional flow—which are measured using different devices or rheometers. The properties are better studied using tensor-valued constitutive equations, which are common in the field of continuum mechanics [2].

Peristaltic pumping has been the object of scientific and engineering research in recent years. The word peristaltic comes from a Greek word "Peristaltikos" which means clasp and compressing. The peristaltic transport is traveling contraction wave along a tube-like structure, and it results physiologically from neuron-muscular properties of any tubular smooth muscle. Peristaltic motion of blood (or other fluid) in animal or human bodies have been considered by many authors. It is well known that peristaltic flow is generated by means of moving contraction on the tube and channel walls. The mechanism of peristalsis is used in the body for pumping physiological fluids from one place to another [1,2]. Due to indispensable role of peristaltic flows, it has been extensively studied in both mechanical and physiological situations under different conditions. Recently, several studies are being made on the peristaltic motion of Newtonian and non-Newtonian fluids. Moreover, the study of hydrodynamics has gained very much attention within the more general context of magnetohydrodynamics (MHD) in the last few years. The study of the motion of Newtonian and non-Newtonian fluids in the presence as well as in the absence of magnetic field has found several applications in different areas, including the biological fluids and the flow of nuclear fuel slurries, liquid metals, alloys, plasma, mercury amalgams and blood etc. To study the MHD effect on peristaltic flow of biological fluids is very important in connection with certain problems of the movement of conductive physiological fluids, for example the blood and the blood pump machines. Such analysis is of great value in medical research [3]. It is an important mechanism for transporting blood, where the cross-section of the artery is contracted or expanded periodically by the propagation of progressive wave. It plays an indispensable role in transporting many physiological fluids in the body in various situations such as urine transport from the kidney to the bladder through the ureter, transport of spermatozoa in the ducts efferent of the male reproductive tract and the movement of the ovum in the fallopian tubes. The effect of rotation on the peristaltic flow of a micropolar fluid through a porous medium with an external magnetic field, the flow of Williamson fluid in the occurrence of induced magnetic field, the influence of the induced magnetic field and heat transfer on the peristaltic motion of a Jeffrey fluid in an asymmetric channel: closed form solutions are investigated in Literature [3]. Mahmoud *et al.* [4] discussed the effect of the rotation on wave motion through cylindrical bore in a micro polar porous medium. The dynamic behavior of a wet long bone that has been modeled as a piezoelectric hollow cylinder of crystal class is investigated before [5]. Heat and mass transfer in the peristaltic flow of hyperbolic tangent fluid are important even in a Johnson Segalman fluid [6]. Other than papers on heat transfer in common fluids in a highly absorbing medium [7] or micro polar fluids [10] the effects of MHD also are investigated simultaneously [8].

The viscosity of a shear thickening fluid, or dilatant fluid, appears to increase when the shear rate increases. Corn starch dissolved in water is a common example: when stirred slowly it looks milky, when stirred vigorously it feels like a very viscous liquid. A familiar example of the opposite, a shear thinning fluid, or pseudo plastic fluid, is wall paint: The paint should flow readily off the brush when it is being applied to a surface but not drip excessively. Note that all thixotropic fluids are extremely shear thinning, but they are significantly time dependent, whereas the colloidal "shear thinning" fluids respond instantaneously to changes in shear rate. Thus, to avoid confusion, the latter classification is more clearly termed pseudo plastic [9].

Another example of a shear thinning fluid is blood. This application is highly favoured within the body, as it allows the viscosity of blood to decrease with increased shear rate. Fluids that have a linear shear stress/shear strain relationship require a finite yield stress before they begin to flow (the plot of shear stress against shear strain does not pass through the origin). These fluids are called Bingham plastics. Several examples are clay suspensions, drilling mud, toothpaste, mayonnaise, chocolate, and mustard. The surface of a Bingham plastic can hold peaks when it is still. By contrast Newtonian fluids have flat featureless surfaces when still [10-11]. There are also fluids whose strain rate is a function of time. Fluids that require a gradually increasing shear stress to maintain a constant strain rate are referred to as rheopectic. An opposite case of this is a fluid that thins out with time and requires a decreasing stress to maintain a constant strain rate. Many common substances exhibit non-Newtonian flows. These include: soap solutions, cosmetics and toothpaste, food such as butter, cheese, jam, ketchup, mayonnaise, soup, taffy, and yogurt, natural substances such as magma, lava, gums, and extracts such as vanilla extract, biological fluids such as blood, saliva, semen, mucus and synovial fluid, and slurries such as cement slurry and paper pulp, emulsions such as mayonnaise, and some kinds of dispersions. Because of its properties, oobleck is often used in demonstrations that exhibit its unusual behavior. A person may walk on a large tub of oobleck without sinking due to its shear thickening properties, given the individual moves quickly enough to provide enough force with each step to cause the thickening. Also, if oobleck is placed on a large subwoofer driven at a sufficiently high volume, it will thicken and form standing waves in response to low frequency sound waves from the speaker [12-14].

Flubber is a non-Newtonian fluid, easily made from polyvinyl alcohol-based glues and borax. It flows under low stresses but breaks under higher stresses and pressures. This combination of fluid-like and solid-like properties makes it a Maxwell fluid. Its behavior can also be described as being viscoelastic or gelatinous. Another example of this is chilled caramel ice cream topping (so long as it incorporates hydrocolloids such as carrageenan and gellan gum) [15]. The sudden application of force—by stabbing the surface with a finger, for example, or rapidly inverting

the container holding it—causes the fluid to behave like a solid rather than a liquid. This is the "shear thickening" property of this non-Newtonian fluid. More gentle treatment, such as slowly inserting a spoon, will leave it in its liquid state. Trying to jerk the spoon back out again; however, will trigger the return of the temporary solid state. Silly Putty is a silicone polymer based suspension which will flow, bounce, or break depending on strain rate. Plant resin is a viscoelastic solid polymer. When left in a container, it will flow slowly as a liquid to conform to the contours of its container. If struck with greater force, however, it will shatter as a solid. Ketchup is a shear thinning fluid. Shear thinning means that the fluid viscosity decreases with increasing shear stress. In other words, fluid motion is initially difficult at slow rates of deformation, but will flow more freely at high rates [16].

The experimental investigation of thermal loading in mutual fluids [17] are also motivated to investigate the joule heating, and viscous dissipation effects on MHD forced convection flow [12] and Creeping flow [18] in various applications [18-23]. As discussed the influence of radially varying MHD on the peristaltic flow with heat and mass transfer of a third order fluid in a diverging tube [25-27], Eyring–Powell fluid, fractional Maxwell fluids, and a Jeffrey-six constant fluid are important [28]. The peristaltic flow and heat transfer in a porous media with long wave approximation with temperature dependent variable viscosity in a curved channel with compliant walls which wall properties are affected on the MHD peristaltic flow has been discussed [29]. The magnetic field could be applied inclined or with an endoscope are interested and followed by some researchers [30-32]. There have been many theoretical models developed to describe the peristaltic flow in an annulus with heat and mass transfer effects [33-35].

For most of the research the wave shape is sinusoidal. In addition the $Re \ll 1$, wave number are near zero, fluid property are viscoelastic, third order fluid, power law fluid, couple stress fluid, and Casson fluid. The flow geometries are various such as two dimensional channel axi-symmetric tube of varying or uniform cross-section, and Two-layered axi-symmetric tube [36].

The goal of the present research is to study the effect of magnetic field on the peristaltic flow of a third fluid in a channel with radiation. Here the governing equations are nonlinear in nature; we used infinitely long wavelength assumption to obtain linearized system of coupled differential equations which are then solved analytically. Expressions for the pressure gradient, velocity, pressure rise, friction force on the heat transfer are given and discussed. The numerical result displayed by figures and the physical meaning is explained. The results indicate that the effect of the non-dimensional wave amplitude, magnetic field, ratio of relaxation to retardation time, radius ratio and non-dimensional volume flow on peristaltic flow is very pronounced.

EXPERIMENTAL SECTION

We consider the three-dimensional laminar flow of third grade fluid. The inlet fluid temperature is considered to be T_∞ . The thermal radiation effect is retained in the energy equation. Induced magnetic field is not taken into account due to smaller magnetic Reynolds number. Electric field is assumed to be zero. The present boundary layer equation for three-dimensional flow of third grade fluid can be expressed as follows:

$$\text{div } \bar{\mathbf{V}} = 0 \quad (1)$$

$$\rho \frac{d\bar{\mathbf{V}}}{d\bar{t}} = \text{div } \bar{\mathbf{T}} + \mathbf{J} \times \mathbf{B} \quad (2)$$

$$\rho C \frac{dT}{d\bar{t}} = k \nabla^2 T + \mathbf{q}_r \quad (3)$$

where $\frac{d}{d\bar{t}}$ is the material derivative, $\bar{\mathbf{V}}$ is the velocity, ρ is the density, C is the specific heat, \mathbf{J} is the current density, \mathbf{q}_r is the radiative heat, \mathbf{B} is the total magnetic field (the induced magnetic field assumed negligible), T is temperature, and $\bar{\mathbf{T}}$ is the Cauchy stress tensor. The constitutive equation for $\bar{\mathbf{T}}$ in a third order fluid is

$$\bar{\mathbf{T}} = -p\bar{\mathbf{I}} + \bar{\mathbf{S}} \quad (4)$$

where p is the pressure, $\bar{\mathbf{I}}$ is the identity tensor and the extra stress tensor $\bar{\mathbf{S}}$ is given by

$$\bar{\mathbf{S}} = \mu \bar{\mathbf{A}}_1 + \alpha_1 \bar{\mathbf{A}}_2 + \alpha_2 \bar{\mathbf{A}}_1^2 + \beta_1 \bar{\mathbf{A}}_3 + \beta_2 (\bar{\mathbf{A}}_2 \bar{\mathbf{A}}_1 + \bar{\mathbf{A}}_1 \bar{\mathbf{A}}_2) + \beta_3 (\text{tr } \bar{\mathbf{A}}_1^2) \bar{\mathbf{A}}_1 \quad (5)$$

in which μ, α, β are the material constants and the Rivlin–Ericksen tensors (\bar{A}_n) are given through the following relations

$$\bar{A}_1 = (\text{grad } \bar{V}) + (\text{grad } \bar{V})^T \quad (6)$$

\bar{A}_1 , The first-order Rivlin–Ericksen, is a Rivlin–Ericksen temporal evolution of the strain rate tensor such that the derivative translates and rotates with the flow field based on the fluid's velocity and \bar{A}_{ij} , the n -th order Rivlin–Ericksen tensor. Also for $n > 1$

$$\bar{A}_n = \frac{d}{dt} \bar{A}_{n-1} + \bar{A}_{n-1} (\text{grad } \bar{V}) + (\text{grad } \bar{V})^T \bar{A}_{n-1}, \quad n > 1 \quad (7)$$

A second-order fluid is a fluid where the stress tensor is the sum of all tensors that can be formed from the velocity field with up to two derivatives, much as a Newtonian fluid is formed from derivatives up to first order. This model may be obtained from a retarded motion expansion truncated at the second-order. Higher-order tensor may be found iteratively by the expression

$$\bar{A}_n = \frac{d}{dt} \bar{A}_{n-1} + \bar{A}_{n-1} (\text{grad } \bar{V}) + (\text{grad } \bar{V})^T \bar{A}_{n-1}, \quad n > 1 \quad (8)$$

The derivative chosen for this expression depends on convention. The upper-convected time derivative, lower-convected time derivative, and Jaumann derivative are often used. For unsteady two-dimensional flows

$$\bar{V} = [\bar{U}(\bar{X}, \bar{Y}, \bar{t}), \bar{V}(\bar{X}, \bar{Y}, \bar{t}), 0], \quad (9)$$

in which \bar{U}, \bar{V} are the material constants and the Rivlin–Ericksen tensors are given through the previous relations.

$$\mathbf{J} = \partial(\mathbf{E} + \mathbf{V} \times \mathbf{B}), \quad (10)$$

where B_x and B_y are the components of velocity along X and Y directions respectively, t is the dimensional time, g is the acceleration due to gravity, α is the thermal expansion coefficient, σ is the electrical conductivity of the fluid, B_0 is the uniform applied magnetic field, $\tau = (\rho c')_p / (\rho c')_f$ is the ratio of the effective heat capacity of material and heat capacity of the fluid α is the thermal expansion coefficient and β is the coefficient of expansion with concentration and k is the permeable parameter. The radiative heat flux in the X -direction is considered negligible as compared to Y -direction. Hence, by using Rosseland approximation for radiation, the radiative heat flux q_r is given by

$$\mathbf{q}_r = - \frac{16\sigma_B n^2 T^3}{3\kappa} \nabla T \quad (11)$$

where σ and k are the Stefan–Boltzmann constant and the mean absorption coefficient, respectively. We assume that the temperature difference with in the flow is sufficiently small such that the term T^4 in a Taylor series about temperature T_0 .

$$\text{div } \mathbf{B} = 0, \quad (12)$$

where

$$\text{div } \mathbf{B} = 0, \quad (13)$$

in which u and v are the velocity components in the x and y directions respectively. It is also assumed that for the flow under consideration there is no motion of the wall in the longitudinal direction. This assumption constrains the deformation of the wall; it does not necessarily imply that the channel is rigid against longitudinal motions, but is a convenient simplification that can be justified by a more complete analysis. The assumption implies that for the no-slip condition at the wall. Neglecting the displacement currents, the Maxwell equations and the Ohm's law are

$$\text{curl } \mathbf{E} = - \frac{\partial \mathbf{B}}{\partial t}, \quad (14)$$

where σ is the electrical conductivity, μ_m is the magnetic permeability and \mathbf{E} is the electric field. The imposed and induced electrical fields are assumed negligible. Under low magnetic Reynolds number approximation,

$$\mathbf{J} \times \mathbf{B} = -\sigma \mathbf{B}_0^2 \bar{\mathbf{V}}, \quad (15)$$

In the above equations the subscripts indicate the partial derivatives. In the fixed coordinate system, the motion is unsteady because of the moving boundary. However, if observed in a coordinate system moving with the speed c , it can be treated as steady because the boundary shape appears to be stationary. The transformations between the two frames are given by

$$\frac{\partial \bar{U}}{\partial \bar{X}} + \frac{\partial \bar{V}}{\partial \bar{Y}} = 0, \quad (16)$$

where U, V are components of the velocity in the moving coordinate system. The Navier stokes equations are

$$\rho \left(\frac{\partial}{\partial \bar{t}} + \bar{U} \frac{\partial}{\partial \bar{X}} + \bar{V} \frac{\partial}{\partial \bar{Y}} \right) \bar{U} = - \frac{\partial \bar{p}(\bar{X}, \bar{Y}, \bar{t})}{\partial \bar{X}} + \frac{\partial \bar{S}_{\bar{X}\bar{X}}}{\partial \bar{X}} + \frac{\partial \bar{S}_{\bar{X}\bar{Y}}}{\partial \bar{Y}} - \sigma B_0^2 \bar{U}, \quad (17)$$

$$\rho \left(\frac{\partial}{\partial \bar{t}} + \bar{U} \frac{\partial}{\partial \bar{X}} + \bar{V} \frac{\partial}{\partial \bar{Y}} \right) \bar{V} = - \frac{\partial \bar{p}(\bar{X}, \bar{Y}, \bar{t})}{\partial \bar{Y}} + \frac{\partial \bar{S}_{\bar{X}\bar{Y}}}{\partial \bar{X}} + \frac{\partial \bar{S}_{\bar{Y}\bar{Y}}}{\partial \bar{Y}}, \quad (18)$$

introducing the non-dimensional variables

$$\begin{aligned} \bar{S}_{\bar{X}\bar{X}} = & 2\mu \bar{U}_{\bar{X}} + \alpha_1 (2\bar{U}_{\bar{X}\bar{t}} + 2\bar{U}\bar{U}_{\bar{X}\bar{X}} + 2\bar{V}\bar{U}_{\bar{X}\bar{Y}} + 4\bar{U}_{\bar{X}}^2 + 2\bar{V}_{\bar{X}}^2 + 2\bar{V}_{\bar{X}}\bar{U}_{\bar{Y}}) + \alpha_2 (4\bar{U}_{\bar{X}}^2 + \bar{U}_{\bar{Y}}^2 + \bar{V}_{\bar{X}}^2 + 2\bar{V}_{\bar{X}}\bar{U}_{\bar{Y}}) \\ & + \beta_1 (2\bar{U}_{\bar{X}\bar{t}\bar{t}} + 2\bar{U}_{\bar{t}}\bar{U}_{\bar{X}\bar{X}} + 4\bar{U}\bar{U}_{\bar{X}\bar{X}\bar{t}} + 2\bar{V}_{\bar{t}}\bar{U}_{\bar{X}\bar{Y}} + 4\bar{V}\bar{U}_{\bar{X}\bar{Y}\bar{t}} + 12\bar{U}_{\bar{X}}\bar{U}_{\bar{X}\bar{t}} + 6\bar{V}_{\bar{X}}\bar{V}_{\bar{X}\bar{t}} + 2\bar{U}_{\bar{Y}}\bar{V}_{\bar{X}\bar{t}} \\ & + 4\bar{U}_{\bar{Y}\bar{t}}\bar{V}_{\bar{X}} + 14\bar{U}\bar{U}_{\bar{X}}\bar{U}_{\bar{X}\bar{X}} + 12\bar{V}\bar{U}_{\bar{X}}\bar{U}_{\bar{X}\bar{Y}} + 8\bar{U}_{\bar{X}}^3 + 6\bar{U}\bar{V}_{\bar{X}}\bar{U}_{\bar{X}\bar{Y}} + 6\bar{V}\bar{V}_{\bar{X}}\bar{V}_{\bar{X}\bar{Y}} + 4\bar{V}\bar{V}_{\bar{X}}\bar{U}_{\bar{Y}\bar{Y}} \\ & + 6\bar{U}\bar{V}_{\bar{X}}\bar{V}_{\bar{X}\bar{X}} + 2\bar{U}^2\bar{U}_{\bar{X}\bar{X}\bar{X}} + 2\bar{U}\bar{V}\bar{U}_{\bar{X}\bar{X}\bar{X}} + 2\bar{V}\bar{U}_{\bar{Y}}\bar{U}_{\bar{X}\bar{X}} + 2\bar{V}^2\bar{U}_{\bar{X}\bar{X}\bar{Y}} + 2\bar{V}\bar{V}_{\bar{Y}}\bar{U}_{\bar{X}\bar{Y}} + 2\bar{V}\bar{U}_{\bar{Y}}\bar{V}_{\bar{X}\bar{Y}} \\ & + 8\bar{U}_{\bar{Y}}\bar{V}_{\bar{X}}\bar{U}_{\bar{X}} + 2\bar{U}\bar{V}_{\bar{X}\bar{X}}\bar{U}_{\bar{Y}} + 4\bar{U}\bar{V}\bar{U}_{\bar{X}\bar{X}\bar{Y}}) \\ & + \beta_1 (8\bar{U}_{\bar{X}}\bar{U}_{\bar{X}\bar{t}} + 8\bar{U}\bar{V}_{\bar{X}}\bar{U}_{\bar{X}\bar{X}} + 8\bar{V}\bar{U}_{\bar{X}}\bar{U}_{\bar{X}\bar{Y}} + 16\bar{U}_{\bar{X}}^3 + 2\bar{U}_{\bar{Y}}\bar{V}_{\bar{X}\bar{t}} + 2\bar{U}_{\bar{Y}}\bar{U}_{\bar{Y}\bar{t}} + 2\bar{V}_{\bar{X}}\bar{V}_{\bar{X}\bar{t}} + 2\bar{U}\bar{U}_{\bar{Y}}\bar{V}_{\bar{X}\bar{X}} \\ & + 2\bar{U}\bar{V}_{\bar{X}}\bar{V}_{\bar{X}\bar{X}} + 2\bar{V}\bar{U}_{\bar{Y}}\bar{V}_{\bar{Y}\bar{Y}} + 2\bar{V}\bar{V}_{\bar{X}}\bar{V}_{\bar{X}\bar{Y}} + 2\bar{U}\bar{U}_{\bar{Y}}\bar{U}_{\bar{X}\bar{Y}} + 2\bar{U}\bar{V}_{\bar{X}}\bar{U}_{\bar{X}\bar{Y}} + 2\bar{V}\bar{V}_{\bar{X}}\bar{U}_{\bar{Y}\bar{Y}} + 2\bar{V}\bar{U}_{\bar{Y}}\bar{V}_{\bar{X}\bar{Y}} \\ & + 4\bar{V}_{\bar{X}}\bar{U}_{\bar{X}}^2 + 4\bar{U}_{\bar{X}}\bar{U}_{\bar{Y}}^2 + 8\bar{U}_{\bar{Y}}\bar{V}_{\bar{X}}\bar{U}_{\bar{X}} + 2\bar{V}_{\bar{X}}\bar{U}_{\bar{Y}\bar{t}}) \\ & + \beta_3 (2\bar{U}_{\bar{X}}^3 + 4\bar{U}_{\bar{X}}\bar{U}_{\bar{Y}}^2 + 8\bar{U}_{\bar{X}}\bar{V}_{\bar{Y}}^2 + 4\bar{U}_{\bar{X}}\bar{V}_{\bar{X}}^2 + 8\bar{U}_{\bar{Y}}\bar{V}_{\bar{X}}\bar{U}_{\bar{X}}), \quad (19) \end{aligned}$$

and defining the stream function $\Psi(x,y)$ through

$$\begin{aligned} \bar{S}_{\bar{X}\bar{Y}} = & \mu (\bar{U}_{\bar{Y}} + \bar{V}_{\bar{X}}) + \alpha_1 (\bar{V}_{\bar{X}\bar{t}} + \bar{U}_{\bar{Y}\bar{t}} + \bar{U}\bar{U}_{\bar{X}\bar{X}} + \bar{V}\bar{V}_{\bar{X}\bar{Y}} + \bar{V}\bar{U}_{\bar{Y}\bar{Y}} + \bar{U}\bar{V}_{\bar{X}\bar{X}} + 2\bar{U}_{\bar{X}}\bar{U}_{\bar{Y}} + \bar{V}_{\bar{X}}\bar{V}_{\bar{Y}}) \\ & + \alpha_1 (2\bar{U}_{\bar{X}}\bar{V}_{\bar{X}} + 2\bar{V}_{\bar{X}}\bar{V}_{\bar{Y}}) \\ & + \beta_1 (\bar{V}_{\bar{X}\bar{t}\bar{t}} + \bar{U}_{\bar{Y}\bar{t}\bar{t}} + \bar{U}_{\bar{t}}\bar{U}_{\bar{X}\bar{Y}} + \bar{U}\bar{U}_{\bar{X}\bar{Y}\bar{t}} + \bar{V}_{\bar{t}}\bar{V}_{\bar{X}\bar{Y}} + 2\bar{V}\bar{V}_{\bar{X}\bar{Y}\bar{t}} + 2\bar{V}\bar{U}_{\bar{Y}\bar{Y}\bar{t}} + \bar{V}_{\bar{t}}\bar{U}_{\bar{Y}\bar{Y}} + \bar{U}_{\bar{t}}\bar{V}_{\bar{X}\bar{X}} \\ & + 2\bar{U}\bar{V}_{\bar{X}\bar{X}\bar{t}} + 2\bar{V}_{\bar{Y}}\bar{V}_{\bar{X}\bar{t}} + 4\bar{V}_{\bar{X}}\bar{V}_{\bar{Y}\bar{t}} + \bar{V}_{\bar{Y}}\bar{V}_{\bar{Y}\bar{t}} + 4\bar{U}_{\bar{X}\bar{t}}\bar{U}_{\bar{Y}} + 3\bar{U}_{\bar{X}}\bar{U}_{\bar{Y}\bar{t}} + 5\bar{V}_{\bar{Y}}\bar{U}_{\bar{X}\bar{Y}} + 4\bar{U}\bar{U}_{\bar{Y}}\bar{U}_{\bar{X}\bar{X}} \\ & + 4\bar{U}_{\bar{X}}^2\bar{U}_{\bar{Y}} + 4\bar{V}_{\bar{X}}^2\bar{U}_{\bar{Y}} + 4\bar{V}_{\bar{X}}\bar{U}_{\bar{Y}}^2 + 2\bar{V}_{\bar{Y}}\bar{U}_{\bar{Y}\bar{Y}} + \bar{U}\bar{V}_{\bar{X}\bar{X}}\bar{V}_{\bar{Y}} + 4\bar{V}_{\bar{X}}\bar{V}_{\bar{Y}}^2 + 4\bar{U}_{\bar{X}}\bar{U}_{\bar{X}\bar{Y}} + 2\bar{V}\bar{V}_{\bar{Y}}\bar{V}_{\bar{X}\bar{X}} + 4\bar{V}\bar{V}_{\bar{X}}\bar{V}_{\bar{Y}\bar{Y}} \\ & + \bar{U}\bar{U}_{\bar{Y}\bar{Y}\bar{t}} + \bar{U}^2\bar{V}_{\bar{X}\bar{X}\bar{X}} + \bar{U}\bar{V}\bar{U}_{\bar{X}\bar{Y}\bar{Y}} + 3\bar{V}\bar{U}_{\bar{X}}\bar{U}_{\bar{Y}\bar{Y}} + 5\bar{U}\bar{V}_{\bar{X}}\bar{V}_{\bar{X}\bar{Y}} + \bar{U}^2\bar{U}_{\bar{X}\bar{X}\bar{Y}} + \bar{U}\bar{V}\bar{V}_{\bar{X}\bar{Y}\bar{Y}} + 2\bar{V}\bar{U}_{\bar{Y}}\bar{U}_{\bar{X}\bar{X}} \\ & + \bar{V}^2\bar{V}_{\bar{X}\bar{Y}\bar{Y}} + \bar{U}\bar{V}\bar{V}_{\bar{X}\bar{X}\bar{Y}} + \bar{U}\bar{V}_{\bar{X}\bar{X}}\bar{U}_{\bar{Y}}) \\ & + \beta_2 (2\bar{U}_{\bar{X}}\bar{V}_{\bar{X}\bar{t}} + 2\bar{U}_{\bar{X}}\bar{U}_{\bar{Y}\bar{t}} + 2\bar{U}\bar{U}_{\bar{X}}\bar{U}_{\bar{X}\bar{Y}} + 2\bar{V}\bar{U}_{\bar{X}}\bar{V}_{\bar{X}\bar{Y}} + 2\bar{V}\bar{U}_{\bar{X}}\bar{U}_{\bar{Y}\bar{Y}} + 2\bar{U}\bar{U}_{\bar{X}}\bar{V}_{\bar{X}\bar{X}} + 2\bar{V}_{\bar{X}}\bar{V}_{\bar{Y}\bar{t}} + 2\bar{U}_{\bar{Y}}\bar{U}_{\bar{X}\bar{t}} \\ & + 2\bar{V}_{\bar{X}}\bar{U}_{\bar{X}\bar{t}} + 2\bar{U}\bar{U}_{\bar{Y}}\bar{V}_{\bar{X}\bar{Y}} + 2\bar{V}\bar{V}_{\bar{X}}\bar{U}_{\bar{X}\bar{Y}} + 2\bar{U}\bar{U}_{\bar{Y}}\bar{U}_{\bar{X}\bar{X}} + 2\bar{V}\bar{U}_{\bar{Y}}\bar{U}_{\bar{X}\bar{Y}} + 2\bar{U}\bar{V}_{\bar{X}}\bar{V}_{\bar{X}\bar{Y}} + 2\bar{V}\bar{U}_{\bar{Y}}\bar{V}_{\bar{Y}\bar{Y}} \\ & + 2\bar{U}\bar{V}_{\bar{X}}\bar{U}_{\bar{X}\bar{X}} + 2\bar{U}\bar{V}_{\bar{Y}}\bar{V}_{\bar{X}\bar{X}} + 6\bar{V}_{\bar{X}}\bar{U}_{\bar{X}}^2 + 2\bar{V}_{\bar{Y}}\bar{U}_{\bar{Y}\bar{t}} + 2\bar{V}_{\bar{Y}}\bar{V}_{\bar{X}\bar{t}} + 2\bar{V}\bar{V}_{\bar{Y}}\bar{V}_{\bar{X}\bar{Y}} + 2\bar{U}\bar{V}_{\bar{Y}}\bar{U}_{\bar{X}\bar{Y}} + 2\bar{V}\bar{V}_{\bar{Y}}\bar{U}_{\bar{Y}\bar{Y}} \\ & + 2\bar{U}_{\bar{X}}^2\bar{U}_{\bar{Y}} + 6\bar{V}_{\bar{X}}^2\bar{U}_{\bar{Y}} + 2\bar{V}_{\bar{X}}^3 + 6\bar{V}_{\bar{X}}\bar{U}_{\bar{Y}}^2 + 6\bar{V}_{\bar{Y}}^2\bar{U}_{\bar{Y}} + 2\bar{V}_{\bar{Y}}^2\bar{V}_{\bar{X}} + 2\bar{U}_{\bar{Y}}\bar{V}_{\bar{Y}\bar{t}}) \\ & + \beta_3 (\bar{U}_{\bar{X}}^3\bar{U}_{\bar{Y}} + 2\bar{U}_{\bar{Y}}^3 + 6\bar{V}_{\bar{X}}^2\bar{U}_{\bar{Y}} + 4\bar{V}_{\bar{Y}}^2\bar{U}_{\bar{Y}} + 6\bar{V}_{\bar{X}}\bar{U}_{\bar{Y}}^2 + \bar{V}_{\bar{X}}\bar{U}_{\bar{X}}^2 + 2\bar{V}_{\bar{X}}^3 + 4\bar{V}_{\bar{Y}}^2\bar{V}_{\bar{X}}), \quad (20) \end{aligned}$$

the continuity equation is identically satisfied and from Eqs (19) and we deduce that

$$\begin{aligned} \bar{S}_{\bar{X}\bar{Y}} = & \mu (\bar{U}_{\bar{Y}} + \bar{V}_{\bar{X}}) + \alpha_1 (\bar{V}_{\bar{X}\bar{t}} + \bar{U}_{\bar{Y}\bar{t}} + \bar{U}\bar{U}_{\bar{X}\bar{X}} + \bar{V}\bar{V}_{\bar{X}\bar{Y}} + \bar{V}\bar{U}_{\bar{Y}\bar{Y}} + \bar{U}\bar{V}_{\bar{X}\bar{X}} + 2\bar{U}_{\bar{X}}\bar{U}_{\bar{Y}} + \bar{V}_{\bar{X}}\bar{V}_{\bar{Y}}) \\ & + \alpha_1 (2\bar{U}_{\bar{X}}\bar{V}_{\bar{X}} + 2\bar{V}_{\bar{X}}\bar{V}_{\bar{Y}}) \\ & + \beta_1 (\bar{V}_{\bar{X}\bar{t}\bar{t}} + \bar{U}_{\bar{Y}\bar{t}\bar{t}} + \bar{U}_{\bar{t}}\bar{U}_{\bar{X}\bar{Y}} + \bar{U}\bar{U}_{\bar{X}\bar{Y}\bar{t}} + \bar{V}_{\bar{t}}\bar{V}_{\bar{X}\bar{Y}} + 2\bar{V}\bar{V}_{\bar{X}\bar{Y}\bar{t}} + 2\bar{V}\bar{U}_{\bar{Y}\bar{Y}\bar{t}} + \bar{V}_{\bar{t}}\bar{U}_{\bar{Y}\bar{Y}} + \bar{U}_{\bar{t}}\bar{V}_{\bar{X}\bar{X}} \\ & + 2\bar{U}\bar{V}_{\bar{X}\bar{X}\bar{t}} + 2\bar{V}_{\bar{Y}}\bar{V}_{\bar{X}\bar{t}} + 4\bar{V}_{\bar{X}}\bar{V}_{\bar{Y}\bar{t}} + \bar{V}_{\bar{Y}}\bar{V}_{\bar{Y}\bar{t}} + 4\bar{U}_{\bar{X}\bar{t}}\bar{U}_{\bar{Y}} + 3\bar{U}_{\bar{X}}\bar{U}_{\bar{Y}\bar{t}} + 5\bar{V}_{\bar{Y}}\bar{U}_{\bar{X}\bar{Y}} + 4\bar{U}\bar{U}_{\bar{Y}}\bar{U}_{\bar{X}\bar{X}} \\ & + 4\bar{U}_{\bar{X}}^2\bar{U}_{\bar{Y}} + 4\bar{V}_{\bar{X}}^2\bar{U}_{\bar{Y}} + 4\bar{V}_{\bar{X}}\bar{U}_{\bar{Y}}^2 + 2\bar{V}_{\bar{Y}}\bar{U}_{\bar{Y}\bar{Y}} + \bar{U}\bar{V}_{\bar{X}\bar{X}}\bar{V}_{\bar{Y}} + 4\bar{V}_{\bar{X}}\bar{V}_{\bar{Y}}^2 + 4\bar{U}_{\bar{X}}\bar{U}_{\bar{X}\bar{Y}} + 2\bar{V}\bar{V}_{\bar{Y}}\bar{V}_{\bar{X}\bar{X}} + 4\bar{V}\bar{V}_{\bar{X}}\bar{V}_{\bar{Y}\bar{Y}} \\ & + \bar{U}\bar{U}_{\bar{Y}\bar{Y}\bar{t}} + \bar{U}^2\bar{V}_{\bar{X}\bar{X}\bar{X}} + \bar{U}\bar{V}\bar{U}_{\bar{X}\bar{Y}\bar{Y}} + 3\bar{V}\bar{U}_{\bar{X}}\bar{U}_{\bar{Y}\bar{Y}} + 5\bar{U}\bar{V}_{\bar{X}}\bar{V}_{\bar{X}\bar{Y}} + \bar{U}^2\bar{U}_{\bar{X}\bar{X}\bar{Y}} + \bar{U}\bar{V}\bar{V}_{\bar{X}\bar{Y}\bar{Y}} + 2\bar{V}\bar{U}_{\bar{Y}}\bar{U}_{\bar{X}\bar{X}} \\ & + \bar{V}^2\bar{V}_{\bar{X}\bar{Y}\bar{Y}} + \bar{U}\bar{V}\bar{V}_{\bar{X}\bar{X}\bar{Y}} + \bar{U}\bar{V}_{\bar{X}\bar{X}}\bar{U}_{\bar{Y}}) \\ & + \beta_2 (2\bar{U}_{\bar{X}}\bar{V}_{\bar{X}\bar{t}} + 2\bar{U}_{\bar{X}}\bar{U}_{\bar{Y}\bar{t}} + 2\bar{U}\bar{U}_{\bar{X}}\bar{U}_{\bar{X}\bar{Y}} + 2\bar{V}\bar{U}_{\bar{X}}\bar{V}_{\bar{X}\bar{Y}} + 2\bar{V}\bar{U}_{\bar{X}}\bar{U}_{\bar{Y}\bar{Y}} + 2\bar{U}\bar{U}_{\bar{X}}\bar{V}_{\bar{X}\bar{X}} + 2\bar{V}_{\bar{X}}\bar{V}_{\bar{Y}\bar{t}} + 2\bar{U}_{\bar{Y}}\bar{U}_{\bar{X}\bar{t}} \\ & + 2\bar{V}_{\bar{X}}\bar{U}_{\bar{X}\bar{t}} + 2\bar{U}\bar{U}_{\bar{Y}}\bar{V}_{\bar{X}\bar{Y}} + 2\bar{V}\bar{V}_{\bar{X}}\bar{U}_{\bar{X}\bar{Y}} + 2\bar{U}\bar{U}_{\bar{Y}}\bar{U}_{\bar{X}\bar{X}} + 2\bar{V}\bar{U}_{\bar{Y}}\bar{U}_{\bar{X}\bar{Y}} + 2\bar{U}\bar{V}_{\bar{X}}\bar{V}_{\bar{X}\bar{Y}} + 2\bar{V}\bar{U}_{\bar{Y}}\bar{V}_{\bar{Y}\bar{Y}} \\ & + 2\bar{U}\bar{V}_{\bar{X}}\bar{U}_{\bar{X}\bar{X}} + 2\bar{U}\bar{V}_{\bar{Y}}\bar{V}_{\bar{X}\bar{X}} + 6\bar{V}_{\bar{X}}\bar{U}_{\bar{X}}^2 + 2\bar{V}_{\bar{Y}}\bar{U}_{\bar{Y}\bar{t}} + 2\bar{V}_{\bar{Y}}\bar{V}_{\bar{X}\bar{t}} + 2\bar{V}\bar{V}_{\bar{Y}}\bar{V}_{\bar{X}\bar{Y}} + 2\bar{U}\bar{V}_{\bar{Y}}\bar{U}_{\bar{X}\bar{Y}} + 2\bar{V}\bar{V}_{\bar{Y}}\bar{U}_{\bar{Y}\bar{Y}} \\ & + 2\bar{U}_{\bar{X}}^2\bar{U}_{\bar{Y}} + 6\bar{V}_{\bar{X}}^2\bar{U}_{\bar{Y}} + 2\bar{V}_{\bar{X}}^3 + 6\bar{V}_{\bar{X}}\bar{U}_{\bar{Y}}^2 + 6\bar{V}_{\bar{Y}}^2\bar{U}_{\bar{Y}} + 2\bar{V}_{\bar{Y}}^2\bar{V}_{\bar{X}} + 2\bar{U}_{\bar{Y}}\bar{V}_{\bar{Y}\bar{t}}) \\ & + \beta_3 (\bar{U}_{\bar{X}}^3\bar{U}_{\bar{Y}} + 2\bar{U}_{\bar{Y}}^3 + 6\bar{V}_{\bar{X}}^2\bar{U}_{\bar{Y}} + 4\bar{V}_{\bar{Y}}^2\bar{U}_{\bar{Y}} + 6\bar{V}_{\bar{X}}\bar{U}_{\bar{Y}}^2 + \bar{V}_{\bar{X}}\bar{U}_{\bar{X}}^2 + 2\bar{V}_{\bar{X}}^3 + 4\bar{V}_{\bar{Y}}^2\bar{V}_{\bar{X}}), \quad (21) \end{aligned}$$

indicates that $p \neq p(y)$ and so by eliminating p from Eqs. (18) and (17), we have the following vorticity transport equation

$$\begin{aligned} \bar{S}_{\bar{y}\bar{y}} = & 2\mu\bar{V}_{\bar{y}} + \alpha_1(2\bar{V}_{\bar{y}\bar{t}} + 2\bar{U}\bar{V}_{\bar{x}\bar{y}} + 2\bar{V}\bar{V}_{\bar{y}\bar{y}} + 2\bar{U}_{\bar{y}}^2 + 4\bar{V}_{\bar{y}}^2 + 2\bar{V}_{\bar{x}}\bar{U}_{\bar{y}}) + \alpha_2(\bar{U}_{\bar{y}}^2 + 4\bar{V}_{\bar{y}}^2 + \bar{V}_{\bar{x}}^2 + 2\bar{V}_{\bar{x}}\bar{U}_{\bar{y}}) \\ & + \beta_1(2\bar{V}_{\bar{y}\bar{t}\bar{t}} + 2\bar{U}_{\bar{t}}\bar{V}_{\bar{x}\bar{y}} + 4\bar{U}\bar{V}_{\bar{x}\bar{y}\bar{t}} + 2\bar{V}_{\bar{t}}\bar{V}_{\bar{y}\bar{y}} + 4\bar{V}\bar{U}_{\bar{y}\bar{t}} + 2\bar{U}_{\bar{y}}\bar{V}_{\bar{x}\bar{t}} + 2\bar{V}_{\bar{x}}\bar{U}_{\bar{y}\bar{t}} + 2\bar{U}_{\bar{y}}\bar{V}_{\bar{x}\bar{t}} + 6\bar{U}_{\bar{y}\bar{t}}\bar{U}_{\bar{y}} \\ & + 12\bar{V}_{\bar{y}}\bar{V}_{\bar{y}\bar{t}} + 4\bar{U}\bar{U}_{\bar{y}}\bar{V}_{\bar{x}\bar{x}} + 6\bar{V}\bar{U}_{\bar{y}}\bar{V}_{\bar{x}\bar{y}} + 8\bar{V}_{\bar{y}}^3 + 6\bar{U}\bar{U}_{\bar{y}}\bar{U}_{\bar{x}\bar{y}} + 6\bar{V}\bar{U}_{\bar{y}}\bar{U}_{\bar{y}\bar{y}} + 12\bar{U}\bar{V}_{\bar{y}}\bar{V}_{\bar{x}\bar{y}} + 14\bar{V}\bar{V}_{\bar{y}}\bar{V}_{\bar{y}\bar{y}} \\ & + 2\bar{U}^2\bar{V}_{\bar{x}\bar{x}\bar{y}} + 4\bar{U}\bar{V}\bar{V}_{\bar{x}\bar{y}\bar{y}} + 2\bar{U}\bar{V}_{\bar{x}}\bar{V}_{\bar{y}\bar{y}} + 2\bar{V}^2\bar{V}_{\bar{y}\bar{y}\bar{y}} + 2\bar{V}\bar{V}_{\bar{y}}\bar{V}_{\bar{x}\bar{y}} + 2\bar{V}\bar{V}_{\bar{x}}\bar{U}_{\bar{y}\bar{y}} + 8\bar{U}_{\bar{y}}\bar{V}_{\bar{y}}\bar{U}_{\bar{x}} \\ & + 2\bar{U}\bar{U}_{\bar{x}\bar{y}}\bar{V}_{\bar{x}}) \\ & + \beta_2(8\bar{V}_{\bar{y}}\bar{V}_{\bar{y}\bar{t}} + 8\bar{U}\bar{V}_{\bar{y}}\bar{V}_{\bar{x}\bar{y}} + 8\bar{V}\bar{V}_{\bar{y}}\bar{V}_{\bar{y}\bar{y}} + 16\bar{V}_{\bar{y}}^3 + 2\bar{U}_{\bar{y}}\bar{V}_{\bar{x}\bar{t}} + 2\bar{U}_{\bar{y}}\bar{U}_{\bar{y}\bar{t}} + 2\bar{V}_{\bar{x}}\bar{V}_{\bar{x}\bar{t}} + 2\bar{V}\bar{U}_{\bar{y}}\bar{V}_{\bar{x}\bar{y}} \\ & + 2\bar{U}\bar{V}_{\bar{x}}\bar{V}_{\bar{x}\bar{x}} + 2\bar{V}\bar{U}_{\bar{y}}\bar{V}_{\bar{x}\bar{x}} + 2\bar{V}\bar{V}_{\bar{x}}\bar{U}_{\bar{y}\bar{y}} + 2\bar{U}\bar{V}_{\bar{x}}\bar{U}_{\bar{x}\bar{y}} + 2\bar{U}\bar{U}_{\bar{y}}\bar{U}_{\bar{x}\bar{y}} + 2\bar{V}\bar{U}_{\bar{y}}\bar{U}_{\bar{y}\bar{y}} + 4\bar{V}_{\bar{y}}\bar{U}_{\bar{y}}^2 + 4\bar{V}_{\bar{y}}\bar{V}_{\bar{x}}^2 \\ & + 8\bar{U}_{\bar{y}}\bar{V}_{\bar{y}}\bar{U}_{\bar{x}} + 2\bar{V}\bar{V}_{\bar{x}}\bar{V}_{\bar{x}\bar{y}} + 2\bar{V}_{\bar{x}}\bar{U}_{\bar{y}\bar{t}}) + \beta_3(8\bar{V}_{\bar{y}}^3 + 2\bar{V}_{\bar{y}}\bar{U}_{\bar{x}}^2 + 4\bar{V}_{\bar{y}}\bar{V}_{\bar{x}}^2 + 4\bar{V}_{\bar{y}}\bar{U}_{\bar{y}}^2 + 8\bar{U}_{\bar{y}}\bar{V}_{\bar{x}}\bar{U}_{\bar{x}}) \end{aligned} \quad (22)$$

Or in the form of sai function:

$$\begin{aligned} S_{yy} = & \lambda_1 \left(-2\delta^3 \frac{\partial \Psi}{\partial y} \frac{\partial^3 \Psi}{\partial x^2 \partial y} + 2\delta^2 \frac{\partial \Psi}{\partial x} \frac{\partial^3 \Psi}{\partial x \partial y^2} + 4\delta^2 \left(\frac{\partial^2 \Psi}{\partial x \partial y} \right) - 2\delta^2 \frac{\partial^2 \Psi}{\partial x^2} \frac{\partial^2 \Psi}{\partial y^2} + 2 \left(\frac{\partial^2 \Psi}{\partial x^2} \right)^2 \right) - 2\delta \frac{\partial^2 \Psi}{\partial x \partial y} \\ & + \lambda_2 \left(\delta^4 \left(\frac{\partial^2 \Psi}{\partial x^2} \right)^2 + 4\delta^2 \left(\frac{\partial^2 \Psi}{\partial x \partial y} \right)^2 - 2\delta^2 \frac{\partial^2 \Psi}{\partial x^2} \frac{\partial^2 \Psi}{\partial y^2} + \left(\frac{\partial^2 \Psi}{\partial y^2} \right)^2 \right) \\ & + \gamma_1 \left[-2\delta^5 \left(\frac{\partial \Psi}{\partial y} \right)^2 \frac{\partial^4 \Psi}{\partial x^3 \partial y} - 2\delta^5 \frac{\partial \Psi}{\partial y} \frac{\partial^2 \Psi}{\partial x \partial y} \frac{\partial^3 \Psi}{\partial x^2 \partial y} + 4\delta^4 \frac{\partial \Psi}{\partial x} \frac{\partial \Psi}{\partial y} \frac{\partial^4 \Psi}{\partial x^2 \partial y^2} + 2\delta^4 \frac{\partial \Psi}{\partial x} \frac{\partial^2 \Psi}{\partial y^2} \frac{\partial^3 \Psi}{\partial x^2 \partial y} \right. \\ & + 2\delta^4 \frac{\partial \Psi}{\partial y} \frac{\partial^2 \Psi}{\partial x^2} \frac{\partial^3 \Psi}{\partial x \partial y^2} - \delta^3 \left(\frac{\partial \Psi}{\partial x} \right)^2 \frac{\partial^4 \Psi}{\partial x \partial y^3} - 2\delta^4 \frac{\partial \Psi}{\partial y} \frac{\partial^2 \Psi}{\partial x^2} \frac{\partial^3 \Psi}{\partial y^2 \partial x} - 12\delta^3 \frac{\partial \Psi}{\partial x} \frac{\partial^2 \Psi}{\partial x \partial y} \frac{\partial^3 \Psi}{\partial y^2 \partial x} \\ & + 12\delta^4 \frac{\partial^2 \Psi}{\partial x \partial y} \frac{\partial \Psi}{\partial y} \frac{\partial^3 \Psi}{\partial x^2 \partial y} - 4\delta^4 \frac{\partial \Psi}{\partial x} \frac{\partial^2 \Psi}{\partial x \partial y} \frac{\partial^3 \Psi}{\partial x^2 \partial y} + 2\delta^3 \frac{\partial \Psi}{\partial x} \frac{\partial^2 \Psi}{\partial x^2} \frac{\partial^3 \Psi}{\partial y^3} - 6\delta \frac{\partial \Psi}{\partial x} \frac{\partial^2 \Psi}{\partial y^2} \frac{\partial^3 \Psi}{\partial y^3} \\ & \left. - 4\delta^4 \frac{\partial \Psi}{\partial y} \frac{\partial^2 \Psi}{\partial y^2} \frac{\partial^3 \Psi}{\partial x^3} + 6\delta^2 \frac{\partial \Psi}{\partial y} \frac{\partial^2 \Psi}{\partial y^2} \frac{\partial^3 \Psi}{\partial x \partial y^2} - 8\delta^2 \left(\frac{\partial^2 \Psi}{\partial x \partial y} \right)^2 \frac{\partial^2 \Psi}{\partial y^2} - 8\delta^3 \left(\frac{\partial^2 \Psi}{\partial x \partial y} \right)^3 \right] \\ & + \gamma_2 \left[-8\delta^3 \frac{\partial^2 \Psi}{\partial x \partial y} \frac{\partial \Psi}{\partial x} \frac{\partial^3 \Psi}{\partial x^2 \partial y} + 8\delta^4 \frac{\partial \Psi}{\partial y} \frac{\partial^2 \Psi}{\partial x \partial y} \frac{\partial^3 \Psi}{\partial x^2 \partial y} + 16\delta^3 \left(\frac{\partial^2 \Psi}{\partial x \partial y} \right)^3 + 4\delta^4 \frac{\partial^2 \Psi}{\partial x \partial y} \left(\frac{\partial^2 \Psi}{\partial x^2} \right)^2 \right. \\ & + 8\delta^2 \left(\frac{\partial^2 \Psi}{\partial x \partial y} \right)^2 \frac{\partial^2 \Psi}{\partial y^2} + 2\delta^2 \frac{\partial \Psi}{\partial y} \frac{\partial^2 \Psi}{\partial y^2} \frac{\partial^3 \Psi}{\partial x \partial y^2} - 2\delta^4 \frac{\partial \Psi}{\partial y} \frac{\partial^2 \Psi}{\partial x^2} \frac{\partial^3 \Psi}{\partial x \partial y^2} + 2\delta \frac{\partial \Psi}{\partial x} \frac{\partial^2 \Psi}{\partial y^2} \frac{\partial^3 \Psi}{\partial y^3} \\ & + \delta^6 \frac{\partial^2 \Psi}{\partial x^2} \frac{\partial \Psi}{\partial y} \frac{\partial^3 \Psi}{\partial x^3} - 2\delta^5 \frac{\partial \Psi}{\partial x} \frac{\partial^2 \Psi}{\partial x^2} \frac{\partial^3 \Psi}{\partial y \partial x^2} + 2\delta^3 \frac{\partial \Psi}{\partial x} \frac{\partial^2 \Psi}{\partial y^2} \frac{\partial^3 \Psi}{\partial y \partial x^2} + 2\delta^3 \frac{\partial \Psi}{\partial x} \frac{\partial^2 \Psi}{\partial x^2} \frac{\partial^3 \Psi}{\partial y^3} \\ & \left. - 2\delta^4 \frac{\partial \Psi}{\partial y} \frac{\partial^2 \Psi}{\partial y^2} \frac{\partial^3 \Psi}{\partial x^3} + 4\delta^2 \frac{\partial^2 \Psi}{\partial y^2} \left(\frac{\partial^2 \Psi}{\partial x \partial y} \right)^2 \right] \\ & + \gamma_3 \left[-16\delta^3 \left(\frac{\partial^2 \Psi}{\partial x \partial y} \right)^3 + 8\delta^3 \frac{\partial^2 \Psi}{\partial x^2} \frac{\partial^2 \Psi}{\partial y^2} \frac{\partial^2 \Psi}{\partial x \partial y} - 4\delta \frac{\partial^2 \Psi}{\partial x \partial y} \left(\frac{\partial^2 \Psi}{\partial y^2} \right)^2 + 4\delta^5 \frac{\partial^2 \Psi}{\partial x \partial y} \left(\frac{\partial^2 \Psi}{\partial x^2} \right)^2 \right] \end{aligned} \quad (23)$$

where the non-dimensional wave number δ , the Reynolds number Re , the material coefficients and

$$\delta = \frac{2\pi a}{\lambda}, \quad Re = \frac{\rho c a}{\mu}, \quad \lambda_1 = \frac{\alpha_1 c}{\mu a}, \quad \lambda_2 = \frac{\alpha_2 c}{\mu a}, \quad \gamma_1 = \frac{\beta_1 c^2}{\beta a^2} \quad (24)$$

and Hartman number M are given by

$$\gamma_2 = \frac{\beta_2 c^2}{\mu a^2}, \quad \gamma_3 = \frac{\beta_3 c^2}{\mu a^2}, \quad M = \sqrt{\frac{\sigma}{\mu}} B_0 a \quad (25)$$

the solution of above Eq.s is highly complicated, non-linear and thus the closed form solution for arbitrary values of all parameters is impossible. Even the existing solutions for the Newtonian fluid [2] are obtained under one or more assumptions. With this fact in view, we carry out the analysis here for long wavelength. This is a valid assumption especially for the flow of chyme in the small intestine. Long wavelength assumption has already been used by several workers [6], [7], [8] and [9] in the field. For the long wavelength approximation, Eqs. (19-22) give $S_{xx}=S_{yy}=0$, so

$$Re \delta \left[\left(\frac{\partial \Psi}{\partial y} \frac{\partial}{\partial x} - \frac{\partial \Psi}{\partial x} \frac{\partial}{\partial y} \right) \nabla^2 \Psi \right] = \left[\left(\frac{\partial^2}{\partial y^2} + \delta^2 \frac{\partial^2}{\partial x^2} \right) S_{xy} \right] + \delta \left[\frac{\partial^2}{\partial x \partial y} (S_{xx} - S_{xy}) \right] - M^2 \frac{\partial^2 \Psi}{\partial y^2} \quad (26)$$

where the Deborah number and

$$\frac{\partial^4 \Psi}{\partial y^4} = -2\Gamma \frac{\partial^2}{\partial y^2} \left(\frac{\partial^2 \Psi}{\partial y^2} \right)^3 + M^2 \frac{\partial^2 \Psi}{\partial y^2} \quad (27)$$

and $\Gamma = \gamma_2 + \gamma_3$. In the wave frame the non-dimensional boundary conditions are

$$\frac{\partial p}{\partial x} = \frac{\partial^3 \Psi}{\partial y^3} + 2\Gamma \frac{\partial}{\partial y} \left(\frac{\partial^2 \Psi}{\partial y^2} \right)^3 - M^2 \left(\frac{\partial \Psi}{\partial y} + 1 \right) \quad (28)$$

where $S_{xy} = \frac{\partial^2 \Psi}{\partial y^2} + 2\Gamma \left(\frac{\partial^2 \Psi}{\partial y^2} \right)^3$ is the non-dimensional mean flow and non-dimensional surface of the peristaltic wall h becomes $h(x) = 1 + \Delta \sin x$

$$\left. \begin{aligned} \Psi = 0, \quad \frac{\partial^2 \Psi}{\partial y^2} = 0 \text{ at } y = 0, \\ \frac{\partial \Psi}{\partial y} = -1, \quad \Psi = F \text{ at } y = 0, \end{aligned} \right\} \quad (29)$$

in which the amplitude ratio $\Delta (=b/a)$ and $0 < \Delta < 1$.

RESULTS AND DISCUSSION

The boundary value problem consisting is non-linear and it is difficult to get a closed form solution. However for vanishing Γ , the boundary value problem is amenable to an easy analytical solution. In this case the equation becomes linear and can be solved. Vanishing Γ leads to a problem of a Newtonian fluid. However, small Γ suggests the use of perturbation technique to solve the non-linear problem. Consider an incompressible magnetohydrodynamic (MHD) flow of Williamson fluid in a symmetric channel of width $2d_1$. Both the magnetic field and channel are inclined at angles Θ and α . Here x -axis is taken along the length of channel and y -axis transverse to it (see Fig. 1). A uniform magnetic field B is applied. The induced magnetic field is neglected by assuming a very small magnetic Reynolds number. Also the electric field is taken absent. Heat and mass transfer is examined through convective conditions. In above equations τ is the elastic tension in the membrane, m the mass per unit area, the coefficient of viscous damping, B the flexural rigidity of the plate, H the spring stiffness, h_1 the heat transfer coefficient. Analog to the convective conditions at the wall, we have applied the mixed condition for mass transfer as well. Therefore h_2 indicates the mass transfer coefficient in the similar way as the heat transfer (it is a parameter that is used to describe the ratio between actual mass flux of specie into or out of the flowing fluid and the driving force that causes that flux). T_0 and C_0 represent the temperature and concentration at the upper and lower walls respectively. In the above equations $\epsilon = a/d_1$ is the geometric parameter, $\delta = d_1/\lambda$ the wave number, $Re = \rho c d_1/\mu$ the Reynolds number, $Fr = c^2/g d_1$ the Froude number, Ha the Hartman number, the Brinkman number, $Pr = \mu c_p/k$ and $Ec = c^2/T_0 c_p$ the Prandtl and Eckert numbers respectively, $Sc = \mu/\rho D$ the Schmidt number, $Sr = \rho T_0 D K_T/\mu T_m C_0$ the Soret number, $Du = D_m k_T/\nu C_s C_p$ the Dufour number, $B_{i1} = h_1 d_1/k$ the heat transfer Biot number, $\chi_{i1} = h_2 d_1/D$ the mass transfer Biot number. Here asterisks have been omitted for simplicity. We find the exact instead of series solutions for small Weissenberg number such as

$$\Psi = \Psi_0 + We \Psi_1 + O(We^2), \theta = \theta_0 + We \theta_1 + O(We^2), \phi = \phi_0 + We \phi_1 + O(We^2), Z = Z_0 + We Z_1 + O(We^2).$$

If we have considered the zeroth and first order systems only due to the fact that the perturbation parameter is taken small ($We \ll 1$), then the contribution of higher order terms are negligible due to order analysis. Such contribution for higher order systems is very small. The zeroth order term gives major contribution. First order terms have less value when compared with the zeroth order term. It is noted that subsequent terms are smaller. This fact ensures the convergence. In order to avoid length we only consider the solutions up to first order. Upon making use of zeroth-order solution into the first-order system and then solving the resulting problems

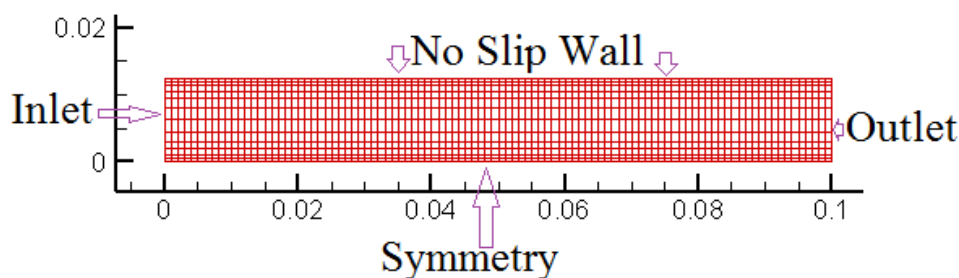


Fig. 1. Boundary condition of problem

In this section, we have presented a set of figures to observe the behavior of sundry parameters involved in the expressions of longitudinal velocity ($u=\psi_{0y}+We\psi_{1y}$), temperature θ , heat transfer coefficient Z and stream function ψ .

Fig. 2, Fig. 3, Fig. 4, Fig. 5 and Fig. 6 display the effects of various physical parameters on the velocity profile $u(x,y)$. Fig. 2 depicts that the velocity increases when thermal radiation enhanced. It is due to the fact that less resistance is offered to the flow because of the wall elastane and thus velocity increases. However reverse effect is observed for Hartman number. As Hartman number represents the damping which is resistive force so velocity decreases when Hartman number is increased. Similar behavior is observed for the velocity in case of rigidity and stiffness due to presence of damping force. Fig. 3 shows that the temperature decreases by increasing Hartman number M . It is due to the fact that magnetic field applied in the transverse direction shows damping effect on the flow. It can be seen that the pumping rate decreases with the increase of α_1 on ΔP with Q for pumping region. While the pumping rate increases as α_1 increase whereas pumping rate increases with increasing the values of β . Fig. 4 illustrates that velocity profile decreases for larger We in the entrance region whereas it has opposite behavior in the outlet region. Since channel exhibits elastic behavior that offers less resistance to flow which in turn speed up the velocity. Due to the fact these figures depict that the velocity for fractional second grade fluid is greater than the second grade fluid. It is observed from Fig. 5 that for subcritical flow ($Fr < 1$) the velocity profile has greater effect than that for critical ($Fr = 1$) and supercritical ($Fr > 1$) flow cases. The velocity profile decreases with an increase of Froude number Fr . It is noted that the pressure rise, the friction forces on the outer tube and the friction forces on the inner tube have a non-zero value only in a bounded region of space. It is observed that the pressure rise decreases with the increasing of the variable magnetic field, the ratio of relaxation to retardation time and radius ratio, as well it increases with increasing of the non-dimensional wave amplitude, while the friction forces on the outer tube and the friction forces on the inner tube increase with increasing of the variable magnetic field, the, the ratio of relaxation to retardation time and radius ratio, as well it decreases with increasing of the non-dimensional wave amplitude. Fig. 6 indicates that the velocity profile is increasing function of the intensity of pressure field. It is observed that in pumping region the pumping increases with an increase of ϕ . However in both free pumping and co-pumping regions this situation is quite opposite to one another. The effect of λ_1 on ΔP with Q indicates that the pumping rate is increasing for time and material constant. It is noted that the pressure gradient has a non-zero value only in a bounded region of space. The effect of the non-dimensional wave amplitude, magnetic field, ratio of relaxation to retardation time, radius ratio and the non-dimensional volume flow on the absolute value of pressure gradient can found there. It is observed that the absolute value of pressure gradient increases with the increasing of variable magnetic field, ratio of relaxation to retardation time, the radius ratio and non-dimensional volume flow while it decreases with increasing of the wave amplitude at $z < 0.5$, as well it that the absolute value of pressure gradient intersects with the effect of the non-dimensional wave amplitude at $z = 0.5$.

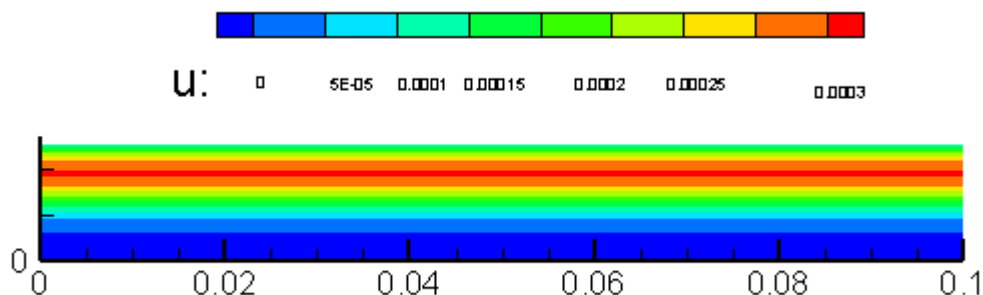


Fig. 2. Effect of thermal radiation on velocity field

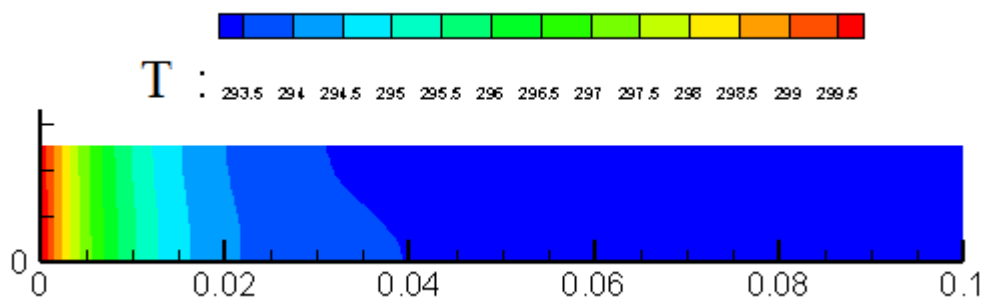


Fig. 3. Effect of thermal radiation on temperature field

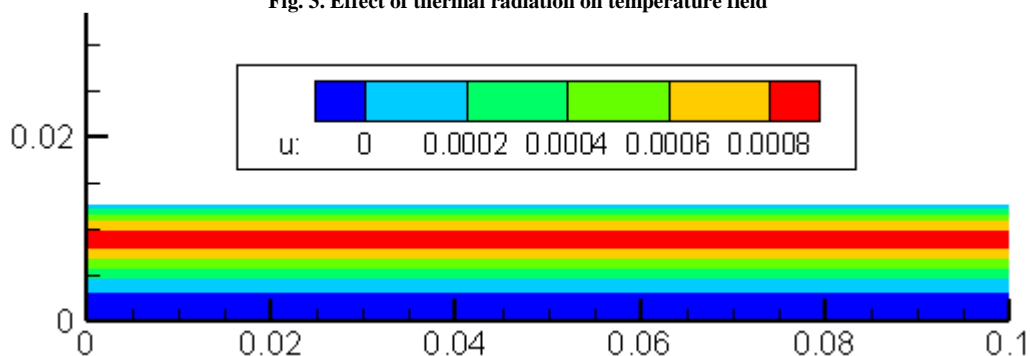


Fig. 4. Effect of Hartman number on velocity field

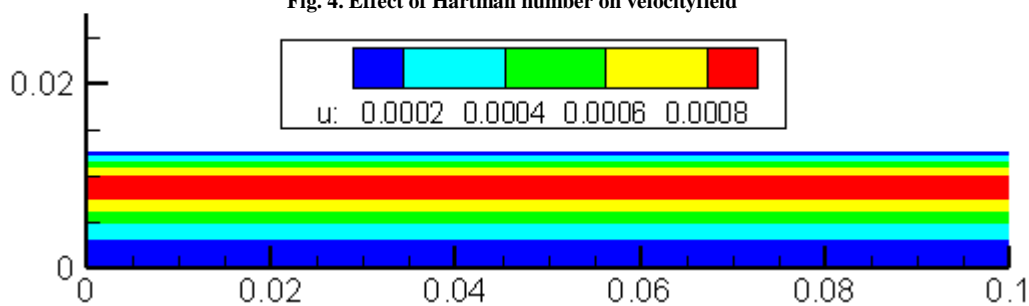


Fig. 5. Effect of amplitude ratio on velocity field

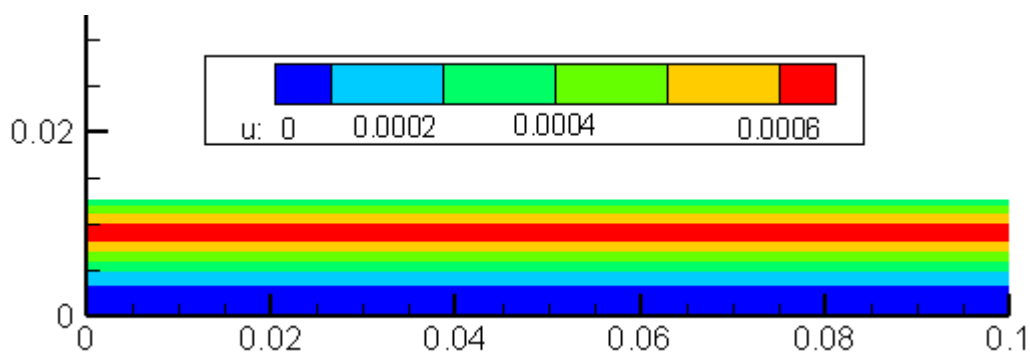


Fig. 6. Effect of intensity of pressure field on velocity field

Fig. 7 and Fig. 8 addressed the variations in temperature distribution for different values of Deborah number β and ratio of relaxation to retardation time λ . Fig. 7 depicts that the temperature is reduced when we use the larger values of Deborah number. The Deborah number β is directly related to relaxation time and this relaxation time is larger for higher Deborah number. Such higher relaxation time creates a reduction in energy due to which temperature field decays. Temperature and thermal boundary layer thickness are increasing functions of ratio of relaxation to retardation times (see Fig. 3). The effect of the non-dimensional wave amplitude, the variable magnetic field, the ratio of relaxation to retardation time, the radius ratio and the non-dimensional volume flow on the absolute value of axial velocity which it decreases and increases gradually. It is observed that the absolute value of axial velocity decreases with increasing of the non-dimensional wave amplitude, magnetic field, ratio of relaxation of retardation time, the radius ratio and the non-dimensional volume flow while it increases with increasing of the all parameters for $z > 0.5$.

The values $\beta=0=\lambda$ correspond to the flow of viscous fluid. Influence of magnetic parameter M on temperature field is analyzed in Fig.9. From this figure we examine that the temperature of hydromagnetic flow ($M>0$) is higher in comparison to hydrodynamic case ($M=0$). The Lorentz force appeared in hydromagnetic flow due to presence of magnetic parameter. The Lorentz force is stronger corresponding to larger magnetic parameter due to which higher temperature and thicker thermal boundary layer thickness are noticed in Fig. 7. Fig. 8 elucidates that the larger values of thermal radiation parameter correspond to higher temperature and thicker thermal boundary layer thickness. Physically, the fluid absorbs more heat when we give rise to thermal radiation parameter due to which both temperature and its associated boundary layer thickness are enhanced. From Fig. 9, we investigated that the temperature and thermal boundary layer thickness are lower for smaller values of thermal radiation parameter and corresponds to the case when thermal radiation is not present. When thermal heat radiation parameter is increased, more heat is produced due to which temperature and boundary layer thickness is higher. It is found that an increase in constant of fractional second grade fluid results in the decrease of velocity profile for the case of fractional second grade fluid. But we noticed that velocity remains unchanged for the case of second grade fluid. The variation of heat transfer coefficient has been presented in Fig. 6. It is interesting to note that the absolute value of heat transfer coefficient increases with an increase in β and ϕ . It is noticed that the nature of heat transfer is oscillatory. This is accordance with the physical expectation due to oscillatory nature of the tube wall. Fig. 7 presents the change in temperature field corresponding to different values of thermal radiation parameter. We have seen that the larger values of thermal radiation parameter lead to higher temperature and thicker thermal boundary layer thickness. Thermal radiation parameter depends on heat transfer coefficient which is stronger for larger thermal radiation parameter that shows higher temperature. The impacts of thermal radiation parameter on the temperature profile are explored in Fig. 8 and Fig. 9. These figures clearly elucidate that the temperature and thermal boundary layer thickness are higher for the larger thermal radiation parameter. Such parameters appeared due to presence of radiation. The presence of thermal radiation enhance the thermal conductivity of fluid due to which higher temperature and thicker thermal boundary layer thickness are observed in Fig. 8 and Fig. 9. From Fig. 10, we examined that an increase in Prandtl number Pr creates a reduction in the temperature field. Physically larger Prandtl number has weaker thermal diffusivity due to which lower temperature is noticed in Fig. 10.

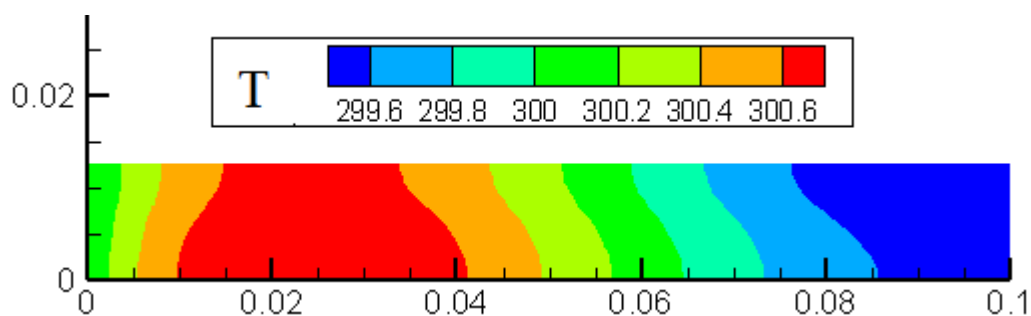


Fig. 7. Effect of thermal radiation on temperature field

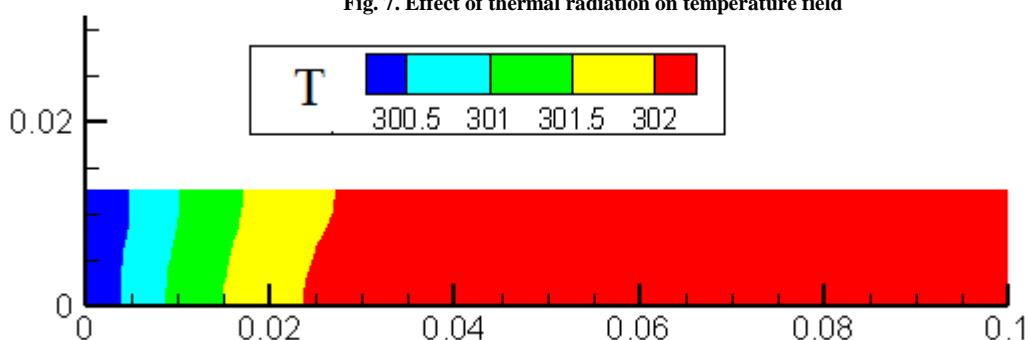


Fig. 8. Thermal boundary layer thickness for the larger thermal radiation parameter

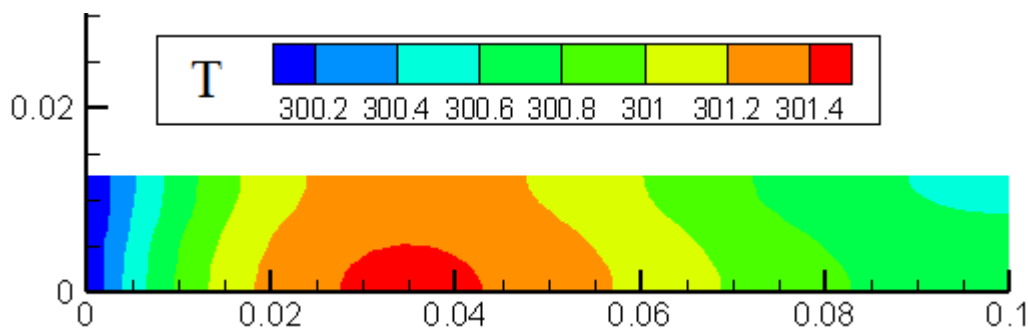


Fig. 9. Influence of magnetic parameter M on temperature field

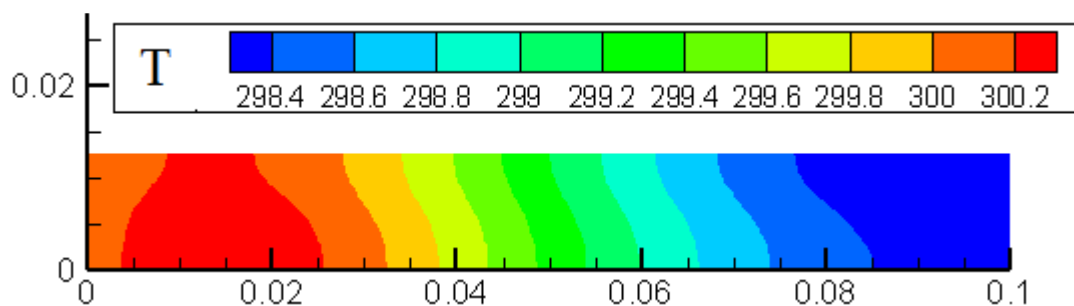


Fig. 10. Effect of Prandtl number on temperature field

CONCLUSION

In this letter, we derived and analyzed a mathematical model subject to low Reynolds number and long wavelength approximations in order to study the peristaltic motion of fractional second grade fluid, the impacts of magnetic field and thermal radiation in a horizontal tube. Analysis has been carried out in the presence of heat transfer and magnetic field. Exact expressions for velocity field, temperature, and averaged flow rate and heat transfer coefficient are obtained. The results extracted are compatible with the physical expectations and are found to satisfy all the subjected conditions. A side by side comparative analysis is performed to compare our findings between second grade fluid and fractional second grade fluid. Moreover, fractional second grade fluid model reduces to second grade fluid models for $\alpha_1 = 1$ and classical Navier Stokes fluid model can be deduced from this as a special case. This provides a useful accuracy check about the correctness and validity of our results and provides a strong confidence into the presented mathematical descriptions. We have seen that the thermal boundary layer thickness is thicker in case of hydromagnetic flow ($M > 0$) in comparison to hydrodynamic flow ($M = 0$). Temperature is enhanced for the gradually increasing values of ratio of relaxation to retardation times but it reduces for larger Deborah number. We observed that the presence of thermal radiation and thermal radiation give rise to the temperature and thermal boundary layer thickness.

REFERENCES

- [1] MY Abdollahzadeh Jamalabadi, *J Porous Media*, **2015**, 18(9), 843-860.
- [2] MY Abdollahzadeh Jamalabadi; JH Park, *Therm Sci*, **2014**, 94-94
- [3] MY Abdollahzadeh Jamalabadi, *Int J Opt Appl*, **2015**, 5(5), 161-167
- [4] MY Abdollahzadeh Jamalabadi, *Chem Eng Res Des*, **2015**, 102, 407-415
- [5] MY Abdollahzadeh Jamalabadi ; JH Park, *World App Sci Journal* , **2014**, (4)32 , 672-677
- [6] MY Abdollahzadeh Jamalabadi; JH Park ; CY Lee, *entropy*, **2015**, 17(2), 866-881
- [7] A Shahidian; M Ghassemi; S Khorasanizade; M Abdollahzade; G Ahmadi, *IEEE Trans Magn*, **2009**, 45(6)2667-2670
- [8] MY Abdollahzadeh Jamalabadi, *J. Marine Sci & App*, **2014**, 13(3) 281-290
- [9] MY Abdollahzadeh Jamalabadi ; JH Park, *Int J. Sci Basic App Res Sci 1* , **2014**, 421-427
- [10] MY Abdollahzadeh Jamalabadi ; JH Park, *Open J. Fluid Dyn*, **2014**, 23(4) 125-132
- [11] MY Abdollahzadeh Jamalabadi; JH Park; MM Rashidi ; JM Chen, *J. Hydrod Ser. B*, **2016**
- [12] MY Abdollahzadeh Jamalabadi, *Front Heat Mass Trans*, **2015**, 6, 013007
- [13] M.Y. Abdollahzadeh Jamalabadi, *J. Fuel Cell Sci. Technol*, **2013**, 10(5), 1039
- [14] MY Abdollahzadeh Jamalabadi; JH Park; CY Lee, *Therm Sci*, **2014**, 124-124
- [15] M Jamalabadi; P Hooshmand; B Khezri ; A Radmanesh, *Ind J sci Res 2* , **2014**, 74-81
- [16] MY Abdollahzadeh Jamalabadi, *Mul Model Mat Struc* , **2016**

- [17] M.Y. Abdollahzadeh Jamalabadi, J.H.Park,C.Y. Lee, *International Journal of Applied Environmental Sciences*, **2014**, 9 (4) 1769-1781
- [18] MY Abdollahzadeh Jamalabadi, *World App. Sci. J.* **2014**, 32 (4) 667-671
- [19] MY Abdollahzadeh Jamalabadi, *Mid-East J. Sci Res* **2014**, 22 (4)561-574
- [20] MY Abdollahzadeh Jamalabadi, *Mat . Perf. Char*, **2015** 20140062
- [21] MS Shadloo; R Poultangari; MY Abdollahzadeh Jamalabadi, MM Rashidi, *Energy Conversion and Management*, **2015**,96 , 418-429
- [22] MY Abdollahzadeh Jamalabadi; M Ghasemi; MH Hamed , *Int J Numer Meth Heat Fluid Flow*,**2013**, 23 (4) 649-661
- [23] MY Abdollahzadeh Jamalabadi, *Int J Ener Mat Chem Pro*,**2016** 15,
DOI:10.1615/IntJEnergeticMaterialsChemProp.2015014428
- [24] MY Abdollahzadeh Jamalabadi, *Noise and Vibration Worldwide*,**2014**, 45 (8) 21-27
- [25] MY Abdollahzadeh Jamalabadi, *J. King Saud Univ Eng Sci*,**2014**, 26 (2) 159-167
- [26] MY Abdollahzadeh Jamalabadi ; M Ghasemi ;MH Hamed, Proc Inst Mech Eng, Part C, *J. Mech Eng Sci*,**2012** ,(226) 1302-1308
- [27] M.Y. Abdollahzadeh Jamalabadi, *Int J Ener Eng*, **2015**, 5(1) 1-8
- [28] M.Y. Abdollahzadeh Jamalabadi, *Int J Mult Res Dev*,**2014**, (1) 5 ,1-4
- [29] S Dousti; J Cao; A Younan; P Allaire; T Dimond, *J. tribology* , **2012**,134 (3), 031704.
- [30] S Dousti; JA Kaplan, F He; PE Allaire, *ASME Turb Exp Conf* , **2013**.
- [31] F He; PE Allaire; S Dousti; A Untaroiu , *ASME Int Mech Eng Cong Exp*, **2013**.
- [32] S Dousti; RL Fittro, *ASME Turb Exp Conf* , **2015**.
- [33] E Sarshari; N Vasegh;M. Khaghani; S Dousti, *ASME Int Mech Eng Cong Exp*, **2013**.
- [34] S Dousti; TW Dimond; PE Allaire, HE Wood, *ASME Int Mech Eng Cong Exp*, **2013**.
- [35] S Dousti;MA Jalali, *J. App Mech*, **2013**, 80 (1), 011019.
- [36] S Bitar; MY Abdollahzadeh Jamalabadi, MY; M Mesbah, *J. Chem. Pharm. Res.*, **2015**, 7(11):91-98
- [37] MY Abdollahzadeh Jamalabadi, *Int J of Eng and App Sci*, **2015**, 7 (5)
- [38] MY Abdollahzadeh Jamalabadi; M Dousti; H Jafarzadeh; F Dadgostari, *Int. J Eng & Adv Tech*, **2015**, 5 (2): 118-124
- [39] MY Abdollahzadeh Jamalabadi, *J of Nig Math Soc*, **2016**
- [40] MY Abdollahzadeh Jamalabadi; S Dousti;*J. Chem. Pharm. Res.*, **2015**, 7(12)